Published in final edited form as:
Biomacromolecules. 2011 December 12; 12(12): 4178–4182. doi:10.1021/bm201214r.

Rapid, high resolution screening of biomaterial hydrogelators by μ^2rheology

Kelly M. Schultz[†], **Alexandra V. Bayles**[†], **Aaron D. Baldwin**[‡], **Kristi L. Kiick**[‡], and **Eric M. Furst**[*,†]
Department of Chemical Engineering and Center for Molecular and Engineering Thermodynamics, University of Delaware, 150 Academy St., Newark, DE 19716, USA, and Department of Materials Science and Engineering and Delaware Biotechnology Institute, University of Delaware, 201 DuPont Hall, Newark, DE 19716, USA

Abstract

A combination of sample manipulation and rheological characterization at the micro-scale is used to identify the gelation of poly(ethylene glycol)-heparin hydrogels over a wide range of compositions. A microfluidic device produces 50–100 droplet samples, each with a different composition. Multiple particle tracking microrheology is used to measure the rheological state of each sample. This combination requires little material and enables efficient and rapid screening of gelation conditions. The high resolution data identifies the gelation reaction percolation boundaries and a lower limit of the total hydrogelator concentration for gelation to occur, which can be used for the subsequent engineering, testing and processing of these materials.

Introduction

Micro-scale sample processing and testing has long been used in interdisciplinary biological research. As far back as a century ago, measurements of cytosol viscosity *in vivo* were enabled by measuring the motion of colloidal nickel particles in the field generated by a strong electromagnet. [1–3] In recent years, high-throughput micro-scale techniques have expanded rapidly to include measurements of polymer properties,[4–9] protein unfolding,[10] solvent-responsive materials[11] and single cells.[12] Not only are these micro-scale approaches the basis of “lab on a chip” concepts,[13–15] but they are increasingly important for characterizing difficult to synthesize or procure materials, including newly identified or engineered biomaterials and biological therapeutics, by expanding the amount of data that can be collected from limited sample quantities.

Biomaterial hydrogelators engineered for therapeutic applications, including drug delivery[16–21] and tissue scaffolds,[22–25] are a class of emerging materials that have benefited from these latter strengths of micro-scale characterization. Efficient, high-throughput measurements are desirable due to the large composition space of these materials, a complexity that arises due to the number of biochemical and biophysical cues that a hydrogel must present to elicit proper cellular function and cell fate. For instance, in tissue scaffolds such cues include adhesion ligands, proteolytic degradation sites, sequestered soluble proteins, including growth factors, as well as the macromolecular structure of the

furst@udel.edu.
[†]Department of Chemical Engineering and Center for Molecular and Engineering Thermodynamics, University of Delaware, 150 Academy St., Newark, DE 19716, USA
[‡]Department of Materials Science and Engineering and Delaware Biotechnology Institute, University of Delaware, 201 DuPont Hall, Newark, DE 19716, USA

hydrogel itself.[26,27] Recently, we demonstrated that microrheology, which uses the Brownian dynamics of colloidal tracer particles dispersed in a sample to measure its rheology, can be employed to characterize the gelation of complex biomaterial hydrogelators.[28,29] Microrheology provides a means to determine the hydrogelator compositions that form gels, the kinetics of gelation and structural information that arises from details of the corresponding percolation transition. [30] A chief advantage of microrheology is the ability to characterize many samples over a range of compositions with relatively little material. Microrheology samples can also be processed in parallel, adding the advantage of an increased rate of data collection.

Here, we demonstrate that significantly higher throughput and resolution of biomaterial hydrogel microrheology is achieved by combining microrheology and microfludics, a method we call μ^2 rheology. Using drop breakup in a microfluidic device, 50–100 microrheology samples are produced in an immiscible, inert carrier fluid. By controlling the inlet flow rates, each droplet sample is made with a unique composition. The samples are sealed in the device and equilibrated in parallel, after which multiple particle tracking microrheology is used to measure the rheology. The resulting high resolution data identifies gel compositions, including the percolation boundaries and a lower limit of the total hydrogelator concentration for gelation to occur, which can be used for the subsequent engineering and processing of these hydrogelators.

Experimental methods

Hydrogel material and solution preparation

The hydrogelator consists of bifunctional 3-mercaptopropionic acid esterified polyethylene glycol (PEG, M_n 5 000) that reacts with multifunctional maleimide-functionalized high molecular weight heparin (HMWH, M_n 15 000). PEG is chosen due to its low immunogenicity and clearance *in vivo*,[31] while HMWH has a unique ability to sequester and stabilize soluble proteins, such as growth factors, which play a vital role in chemical signaling to cells in artificial scaffolds.[32] The PEG and HMWH functionalization chemistries are described in detail elsewhere.[33] The PEG cross-linker is functionalized with two end-terminal thiol groups (functionality, $f_{PEG} = 2$) and the HMWH backbone is functionalized with maleimide groups with an average functionality determined by ^{1}H NMR spectroscopy of $f_{HMWH} = 7.7$.[33]

Solutions of the cross-linker and backbone are prepared in separate 1× phosphate buffered saline (PBS, cat. no. 21-030-CV, Invitrogen). 400 μL solutions are prepared at different concentrations for each dilution experiment, which will fill at least two microfluidic chips. 1.0 μm diameter fluorescent polystyrene latex tracer particles ($2a$ = 1:04±0:02 μm, Polysciences) are diluted in the HMWH solutions at a concentration of 0.054 wt%. The probe particles exhibit good stability in HMWH solutions (they are well dispersed and do not form aggregates). Each solution is loaded into a syringe and attached to the microfluidic device, which is described below. After the samples are created and sealed in the microfluidic channel, they are allowed to equilibrate for at least 2 hours prior to making microrheological measurements. This curing time is chosen because oscillatory rheological measurements show complete gelation well within this period.

Microfluidic device fabrication and sample preparation

The details of the microfluidic device fabrication and theory of operation and operating regimes are described in detail in a recent publication.[34] Here, we briefly review key aspects of the fabrication and implementation of μ^2 rheology.

We fabricate microfluidic channels in a poly(dimethylsiloxane) elastomer (PDMS, Dow Corning) bonded to a custom manufactured glass coverslip slide (75×50×0.15 mm, Thermo Fisher Scientific, Inc.) Sol-gel chemistry using the precursors tetraethoxysilane (TEOS) and methyltriethoxysilane (MTES) is used to create a glass-like silica layer inside the channels to prevent solvent uptake into the PDMS while the hydrogel samples equilibrate.[35] The chemistry of the channel walls are then made hydrophobic by silanization chemistry (0.5% octadecyltrichlorosilane in hexadecane).[36] The final channel is approximately 1.8 mm wide and 0.8 mm high.

The microfluidic device, shown in Figure 1, consists of three inlet streams, a T-junction and a single sample storage channel. Samples are produced within the microfluidic device using pumping programs. A linear gradient of sample concentration is made by alternating the flow rates of the two input streams while maintaing a total sample flow rate of $Q_s = Q_{HMWH} + Q_{PEG} = 5$mL/hr. The HMWH solution decreases from an initially higher volumetric flow rate while the PEG solution flow rate is simultaneously increased over the same period of time. The time to fill the storage channel, approximately 2 minutes, is chosen such that each sample droplet is well mixed and the filling time is much less than the time of gelation, $t_{gel} \approx 5$ minutes. The sample flow is broken into droplets, each with a distinct composition, in a continuous spacer fluid, silicone oil, using a T-junction geometry. Silicone oil is used because it does not react with the hydrogelator and for its high interfacial tension between the oil and the aqueous samples. The oil flow rate is $Q_{oil} = 2.5$mL/hr such that the ratio $(Q_{HMWH}+Q_{PEG})/Q_{oil} = 2$, which ensures that drop breakup occurs in a "pinching" regime and provides optimal spacing and aspect ratio of the droplets.[37] The flow rates are selected such that the droplets have a volume of approximately 3–5 μL, or roughly 1mm in each dimension. This size enables multiple measurements within each droplet of probe particles while limiting the hydrodynamic interactions with the sample boundaries. We estimate that the hindered particle mobility is between 0:1 – 0:4% for particles with diameters of 1 and 3 μm, respectively.[34]

Each droplet sample has a constant weight percent within each microfluidic device. The concentration of each sample drop, C_{An}, is determined by image analysis of the microfluidic device and calculated using

$$C_{An} = \frac{C_{A0} h}{Q_s t_{fill}} \left(a_n \sum_{i=1}^{n-1} A_i + \frac{1}{2} A_n \right) \quad (1)$$

where C_{A0} is the initial concentration, h is the height of the channel, t_{fill} is the total filling time and A_n is the area of each droplet. In this equation, $a_n = 0$ for $n=1$ and $a_n = 1$ for $n>1$. Eight separate microfluidic devices are used to produce samples containing 1% to 8 wt% total polymer to create a gelation state diagram. It should be noted that some material will be lost in the connective tubing and syringe, for this system this total approximately 100 μL total per microfluidic device.

Multiple particle tracking microrheology

Multiple particle tracking microrheology measurements are taken for each equilibrated sample within the microfluidic device. Fluorescent video microscopy (Phantom v5.1, 30 fps, exposure time φ=1 ms) is used to capture the movement of the polystyrene probe particles within the device at a magnification of 63 × (63 × water immersion objective, NA 1.2, 1 × optovar, Carl Zeiss, Inc.). After each movie is taken, the stage is advanced to the next sample and focused by hand. This is done while the movie is being saved and thus requires

no additional time. The exposure time and frame rate are chosen to minimize static and dynamic particle tracking errors.[38] Probe particles are tracked using a brightness-weighted centroid particle tracking algorithm.[39,40] Approximately 100 particles are tracked within each 800 frame movie.

The ensemble-averaged mean-squared displacement (MSD), $\langle \Delta r^2(\tau) \rangle$, of the particles is calculated from the probe particle trajectories. The generalized Stokes-Einstein relation (GSER) is used to directly relate the MSD to the material rheological properties by

$$J(\tau) = \frac{\pi a}{kT} \langle \Delta r^2(\tau) \rangle \quad (2)$$

where $J(\tau)$ is the material creep complaince, τ is the lag time, kT is the thermal energy, and a is the probe particle radius. In the limit of a material with Newtonian viscosity η, $J(\tau) = \tau/\eta$, while an elastic solid with modulus G_0 gives $J = 1=G_0$. Thus, the logarithmic slope of the MSD, $\alpha = d\ln\langle \Delta r^2(\tau) \rangle / d\ln \tau$, can be used to identify the state of the material, i.e. gel or sol; for a Newtonian fluid, $\alpha = 1$ and for an elastic solid, $\alpha = 0$.[30,41] The critical relaxation exponent n of the material is the value of α at the percolation transition, since the time dependence of the incipient gel structure compliance is $J_c \times \tau^n$. Thus, comparing the measured value of α to n identifies the equilibrated sample state as sol or gel; the criteria for a liquid is $\alpha > n$ and for a gel is $\alpha < n$. The value of the critical relaxation exponent is determined previously from time-cure superposition of rheological measurements made during the hydrogelation reaction.[29] For PEG-HMWH hydrogels, the critical relaxation exponent ranges between $0{:}4 \leq n \leq 0{:}6$ depending on the PEG cross-linker molecular weight. In this work, $n = 0{:}48 \pm 0{:}16$ for the 5 000 molecular weight PEG. Particle tracking error, along with the shortest lag time, τ_{min}, determines the minimum compliance for microrheology, $J_{min} = 6\pi a\varepsilon^2/kT$, where ε is the static tracking error.[34] Typically, $\varepsilon \angle 10$ nm. Finally, probe particles sometimes sediment in fluid samples over the two hour sample cure time. Sample droplets for which too few particles are in the center of the droplet to provide accurate ensemble statistics have been excluded from our analysis, and account for some gaps in the data.

Results and discussion

The μ^2rheology method creates fifty to one hundred samples in a time period that is less than the gelation time of the PEG-HMWH material ($t_{gel} \angle 5$ minutes). Since the maximum residence time of a droplet is well below the gel time, all samples are made prior to gelation and the hydrogel network that forms is not subjected to strong deformations. Mixing, however, is a concern in the microfluidic device. As mentioned previously, the microfluidic devices are engineered to mix each droplet sample passively. Winding channels with rough corners encourage the droplets to mix internally from chaotic flow patterns induced as they pass each corner. The droplets are mixed after they pass through two bends in the channel, resulting in a mixing time of approximately 37 seconds.

Each device generates discrete samples that follow a linear composition profile (decreasing HMWH, increasing PEG) at a single value of the total polymer weight percent. First, we examine results from a device which generates a constant weight percent line for 2 wt% total polymer. Figure 2a shows the constant weight percent line and is color coded to show the gelation transition, where blue colors represent a sol and red colors are a gel. The gray points indicate that these samples are not included in the MSD graphs in Figure 2b and c for clarity.

Two percolation transitions occur as the constant weight percent line is traversed from 2:0 wt% HMWH: wt% PEG to 0:2 wt% HMWH: wt% PEG. The corresponding MSDs are shown in Figure 2b and c, respectively. Beginning with an excess of HMWH, as the PEG cross-linker is added the material transitions from a sol to a gel, Figure 2b. The MSD curves show a rapid change from $\alpha = 1$ to $\alpha = 0$. As the amount of HMWH decreases, a second, reverse gel transition is observed, as shown in Figure 2c. In this case, several samples have a slope close to the critical relaxation exponent, $\alpha \angle n$. These two gel transitions occur in every constant weight percent line, and demarcate the gelation envelope, or the compositions that produce a hydrogel. The high composition resolution achieved using μ^2rheology enables these gel transitions to be captured within the measurements.

The combined results of the μ^2rheology for all polymer concentrations are shown in Figure 3. In this graph we see that μ^2rheology increases the number of samples characterized for each total weight percent line. For this material, we also observe that the hydrogel can either gel or remain in the liquid state. Interestingly, a smooth gradient of the sol-gel transition is not observed, but rather, a clear boundary between a strong gel (red circles) and a viscous liquid (blue circles) is typical. We also note a small region of gel formation at the lowest constant weight percent line tested, 1 wt%. This is the lowest concentration hydrogel yet identified for the PEG-HMWH system, and potentially enables engineering of the hydrogel using a minimal amount of polymer. While the experiments suggest that a gel forms at 8 wt % at very low HMWH concentrations (<1 wt% HMWH), further examination of our microscopy data indicates probe particle aggregation occurs for these compositions. Such aggregation is likely a result of depletion attractions between probe particles at high PEG concentrations. These data points have been excluded from Figure 3.

The empirical gelation state diagram in Figure 3 is compared to Flory-Stockmayer theory.[42–44] Previous gelation state diagrams for PEG-HMWH hydrogels were compared to a modified Flory- Stockmayer theory,[28,29] but the statistical considerations for connectivity in the original theory yield a more accurate description of the gelation limits. Flory-Stockmayer theory is an extension of Flory's original work aimed at predicting the critical extent of reaction for gel formation.[42,45] Stockmayer extended Flory's original theory, which only accounted for tri- and tetrafunctional branched polymeric groups, and generalized it to account for any size and branch functionality.[43] The case that Stockmayer describes that applies to the PEG-HMWH hydrogel is for N f -functional polymers and L bifunctional polymers. Here the f -functional polymer is HMWH (recall $f_{\mathrm{HMWH}} = 7{:}7$) and the bifunctional polymer is PEG. The critical extent of reaction is

$$p_c^2 r = \frac{1}{[1+(f-2)\rho]}. \tag{3}$$

Here, r is the total number of maleimide cross-linkable sites divided by total number of PEG thiol groups,

$$r = \frac{f n_{\mathrm{HMWH}}}{2 n_{\mathrm{PEG}}}, \tag{4}$$

where n_{HMWH} is the moles of HMWH, n_{PEG} is the moles of PEG, and ρ is the total polyfunctional HMWH sites divided by all functional sites on the HMWH (this value is always one in our material).[43]

The critical extent of reaction is used to define the lower and upper borders of the gelation envelope. The lower gelation limit is defined when there is an excess of HMWH. For this case, a maximum extent of reaction is defined as

$$p_{max}=\frac{2n_{\mathrm{PEG}}}{fn_{\mathrm{HMWH}}}. \tag{5}$$

The critical extent of reaction must be less than or equal to the maximum extent of reaction. Substituting this value in for p_c into Equation 3 yields the lower gelation boundary of

$$n_{\mathrm{PEG}} \geq \left(\frac{f}{f-1}\right)\frac{n_{\mathrm{HMWH}}}{2}. \tag{6}$$

Similarly, the upper limit is defined as an excess of PEG functional sites and the maximum extent of reaction then becomes one. The resulting upper limit is

$$n_{\mathrm{PEG}} \leq \frac{f(f-1)}{2}n_{\mathrm{HMWH}}. \tag{7}$$

These boundaries are overlaid onto the gelation state diagrams in Figure 3 and exhibit excellent agreement with the experimental gel boundaries.

The PEG-HMWH hydrogel has a large composition range over which gelation occurs, with boundaries that are in good agreement with Flory-Stockmayer theory. In our previous work, PEG 5 000 also had the fastest gelation kinetics compared to smaller and larger cross-linker sizes.[29] Thus, the efficiency of this cross-linker backbone combination, apparent in the total region of gel formation, allows gels to form at the lowest polymer concentrations in the shortest amounts of time. Depending on the application, this could be a desirable property for engineering a therapeutic hydrogel.

Finally, the first and last samples generated using μ^2rheology are single component solutions of the polymers. Using the Stokes-Einstein relation for the projected two-dimensional MSD, $\langle r^2(\tau)\rangle = (2kT/3\pi a\eta)\,\tau$, the viscosity of pure PEG and HMWH is measured. The values are shown in Figure 4. The viscosity values increase as the concentration is increased, which is expected and the values agree with previous measurements of HMWH taken using μ^2rheology.[34] The increase in HMWH viscosity is consistent with the previously measured overlap concentration, c* = 5:9 wt%. Thus, μ^2rheology not only measures the state of material as a function of concentration, but also yields measurements of the constituent polymers.

Comparing the μ^2rheology measurements with the individual MPT measurements reported earlier, we find good agreement between the techniques. Both measured gelation envelopes agree with Flory-Stockmayer theory, but a higher resolution of this limit is obtained with μ^2rheology, as seen in Figure 3. μ^2rheology may also be inherently more accurate due to the sample preparation process, which minimally disrupts the developing hydrogel structure. As mentioned previously, the μ^2rheology samples take 37 seconds to mix in the microfluidic device and are mixed gently by chaotic flows internal to the droplets caused by the winding channel. When creating samples by hand, they are mixed using a pipette and are then

injected into a sample chamber. This latter method shears the sample, possibly leading to breakage of the growing polymer clusters. The entire process of preparing samples by hand also takes approximately one minute to complete. This delay can cause uneven mixing and cluster breakup as the material is sheared prior to being sealed in the sample chamber. Along with decreasing sample preparation time, this method also uses substantially less material per sample (a factor of 18× less) that results in 20× more samples compared to individual MPT samples for the same amount of material.

Conclusions

In this work, we demonstrated that μ^2rheology enables the characterization of scarce biomaterials by maximizing the number of measurements obtained from a small amount of material. Compared to previous high-throughput measurements that relied on the preparation of individual samples, μ^2rheology enables significantly higher data resolution. Using previous methods, each gelation state diagram consists of 25 discrete samples. In contrast, with μ^2rheology, we produce 590 samples in eight microfluidic devices. Thus, substantially less material is required per sample using μ^2rheology. We calculate the amount of HMWH needed for each sample on average (it is an equivalent amount of cross-linker required but the HMWH is the material with the greatest cost, which necessitates conservation). High-throughput microrheology uses 8.8 mg of HMWH per sample while μ^2rheology uses 0.5 mg per sample. Therefore, using μ^2rheology 20× more samples are made with the same amount of material.

μ^2rheology is a powerful measurement technique that enables the characterization of biomaterials over a large composition space with a high resolution. Overall, this screening aids hydrogel engineering by providing the ability to rapidly identify the material percolation boundaries and lowest gel concentrations, and provides important complementary information for performing targeted bulk measurements to quantitatively measure samples with higher moduli. Moreover, for sufficiently soft gels ($G_0 = 1/J_{\min} \leq kT/6\pi a\,\varepsilon^2 \approx 5$Pa), such as samples near the percolation boundaries, the full frequency dependent rheology can be obtained from multiple particle tracking microrheology.

Acknowledgments

We thank P. T. Spicer, K. T. Beers, S. D. Hudson and J. Vermant for helpful discussions. Funding for this work from the National Science Foundation (grant no. CBET-0730292 and DGE-0221651), the National Institutes of Health (5-P20-RR016472-10) and the Procter and Gamble Company is gratefully acknowledged. K.M.S. acknowledges financial support by the NSF Graduate Research Fellowship Program.

References

1. Heilbronn A. Jahrb Wiss Bot. 1922; 61:284–338.
2. Freundlich H, Seifriz WZ. Phys Chem. 1922; 104:232–261.
3. Seifriz W. J Exp Biol. 1924; 1:431–443.
4. Brocchini S, James K, Tangpasuthadol V, Kohn J. JACS. 1997; 119:4553–4554.
5. Simon CG, Stephens JS, Dorsey SM, Becker ML. Rev Sci Instrum. 2007; 78:072207. [PubMed: 17672738]
6. Simon CG, Lin-Gibson S. Adv Mater. 2010; 23:369–387. [PubMed: 20839249]
7. Harrison C, Cabral JT, Stafford CM, Karim A, Amis EJ. J Micromech Microeng. 2004; 14:153–158.
8. Amis EJ. Nat Mater. 2004; 3:83–85. [PubMed: 14755261]
9. Breedveld V, Pine DJ. J Mater Sci. 2003; 38:4461–4470.
10. Tu RS, Breedveld V. Phys Rev E. 2005; 72:041914.
11. Sato J, Breedveld V. J Rheol. 2006; 50:1–19.

12. Krayer J, Tatic-Lucic S, Neti S. Sensors and Actuators B. 2006; 118:20–27.
13. Whitesides GM, Stroock AD. Phys Today. 2001; 54:42–48.
14. Manz A, Harrison DJ, Verpoote EMJ, Fettinger JC, Paulus A, Ludi H, Widmer HM. J Chromatogr A. 1992; 593:253–258.
15. Ng JM, Gitlin I, Stroock AD, Whitesides GM. Electrophoresis. 2002; 23:3461–3473. [PubMed: 12412113]
16. Peppas NA, Hilt JZ, Khademhosseini A, Langer R. Adv Mater. 2006; 18:1345–1360.
17. Liechty WB, Kryscio DR, Slaughter BV, Peppas NA. Annu Rev Chem Biomol Eng. 2010; 1:149–173.
18. Kiick KL. Soft Matter. 2008; 4:29–37. [PubMed: 19960073]
19. Kiick KL. Science. 2007; 317:1182–1183. [PubMed: 17761873]
20. Kopecek J, Kopeckova P. Adv Drug Delivery Rev. 2010; 62:122–149.
21. West JL, Hubbell JA. Reactive Polym. 1995; 25:139–147.
22. Raeber GP, Lutolf MP, Hubbell JA. Biophys J. 2005; 89:1374–1388. [PubMed: 15923238]
23. Kloxin AM, Kloxin CJ, Bowman CN, Anseth KS. Adv Mater. 2010; 22:3484–3494. [PubMed: 20473984]
24. Lee KY, Mooney DJ. Chem Rev. 2001; 101:1869–1880. [PubMed: 11710233]
25. Heilshorn SC, DiZio KA, Welsh ER, Tirrell DA. Biomaterials. 2003; 24:4245–4252. [PubMed: 12853256]
26. Sakiyama-Elbert SE, Hubbell JAJ. Controlled Release. 2000; 65:389–402.
27. Bryant SJ, Anseth KS. J Biomed Mater Res A. 2003; 64A:70–79. [PubMed: 12483698]
28. Schultz KM, Baldwin AD, Kiick KL, Furst EM. Soft Matter. 2009; 5:740–742. [PubMed: 20046915]
29. Schultz KM, Baldwin AD, Kiick KL, Furst EM. Macromolecules. 2009; 42:5310–5316. [PubMed: 21494422]
30. Larsen TH, Furst EM. Phys Rev Lett. 2008; 100:146001. [PubMed: 18518051]
31. Kienberger F, Pastushenko VP, Kada G, Gruber HJ, Riener C, Schindler H, Hinterdorfer P. Single Mol. 2000; 1:123–128.
32. Nie T, Akins RE Jr, Kiick KL. Acta Biomater. 2009; 5:865–875. [PubMed: 19167277]
33. Nie T, Baldwin A, Yamaguchi N, Kiick KL. J Controlled Release. 2007; 122:287–296.
34. Schultz KM, Furst EM. Lab Chip. 201110.1039/C1LC20376B
35. Abate AR, Lee D, Do T, Holtze C, Weitz DA. Lab Chip. 2008; 8:516–518. [PubMed: 18369504]
36. Xiao H, Liang D, Liu G, Guo M, Xing W, Cheng J. Lab Chip. 2006; 6:1067–1072. [PubMed: 16874380]
37. Garstecki P, Fuerstman MJ, Stone HA, Whitesides GM. Lab Chip. 2006; 6:437–447. [PubMed: 16511628]
38. Savin T, Doyle PS. Biophys J. 2005; 88:623–638. [PubMed: 15533928]
39. Crocker JC, Grier DG. J Colloid Interface Sci. 1996; 179:298–310.
40. Crocker, JC.; Weeks, ER. 2011. http://www.physics.emory.edu/weeks/idl/index.html
41. Veerman C, Rajagopal K, Palla CS, Pochan DJ, Schneider JP, Furst EM. Macromolecules. 2006; 39:6608–6614.
42. Flory PJ. J Am Chem Soc. 1941; 63:3083–3090.
43. Stockmayer WH. J Chem Phys. 1943; 11:45–55.
44. Rubinstein, M.; Colby, RH. Polymer Physics. 1. Oxford University Press; 2003.
45. Flory PJ. J Phy Chem. 1942; 46:132–140.

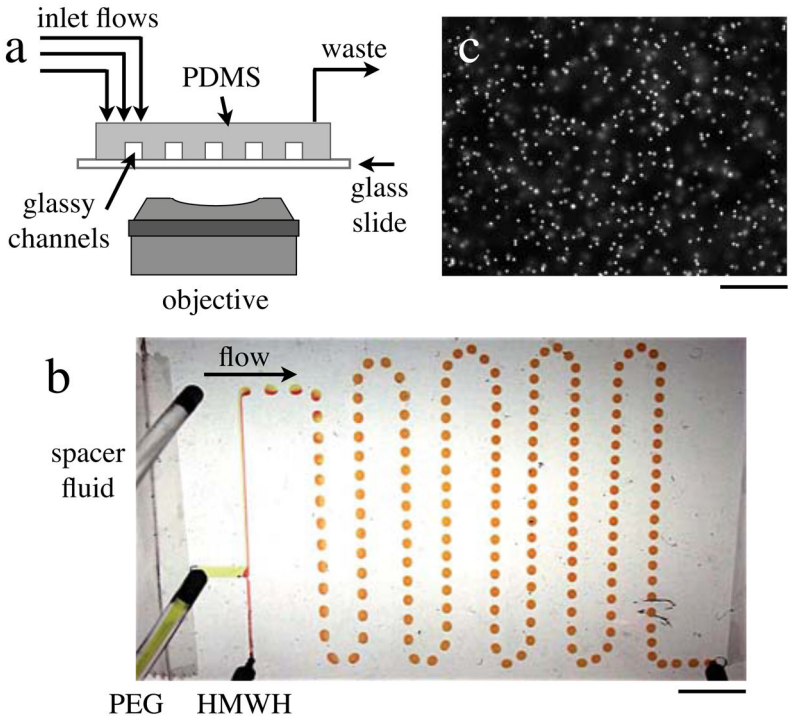

Figure 1.

μ^2rheology measurements combine sample preparation in a microfluidic device with passive microrheological characterization. (a) Microfluidic channels formed in treated PDMS generate 50–100 aqueous droplet samples in an immiscible fluid using a T-junction. (b) The sample streams contain food dyes in this image to aid visualization. After the droplets are made, the device is sealed. The scale bar is 10 mm. (c) Microrheology is performed on each stationary droplet sample by tracking the thermal motion of dispersed fluorescent particles. The scale bar is 25 μm.

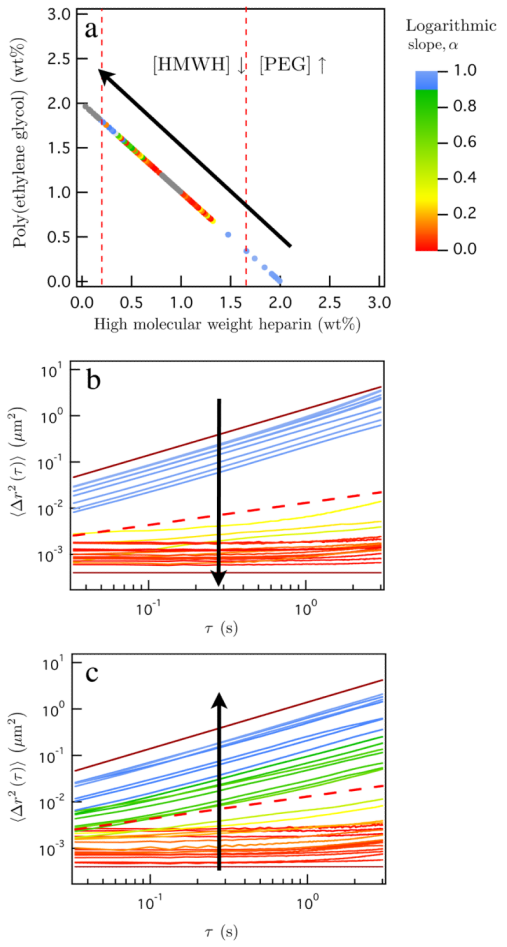

Figure 2.

2 wt% total polymer concentration gel transitions and mean-squared displacements. (a) 2 wt % total polymer line, colors indicate the gel transition where the blue and red symbols indicate a sol and gel, respectively. The red dashed lines indicate the theoretical sol-gel transitions calculated from Flory-Stockmayer theory. (b) Lower gelation transition and (c) upper gelation limit for the sol-gel transitions of the total polymer wt% of 2. The line colors correspond to the color bar on the gelation state diagram. The lower and upper solid lines have slopes 1 and 0, respectively. The dashed line corresponds to the slope set by the critical relaxation exponent, n = 0:48.

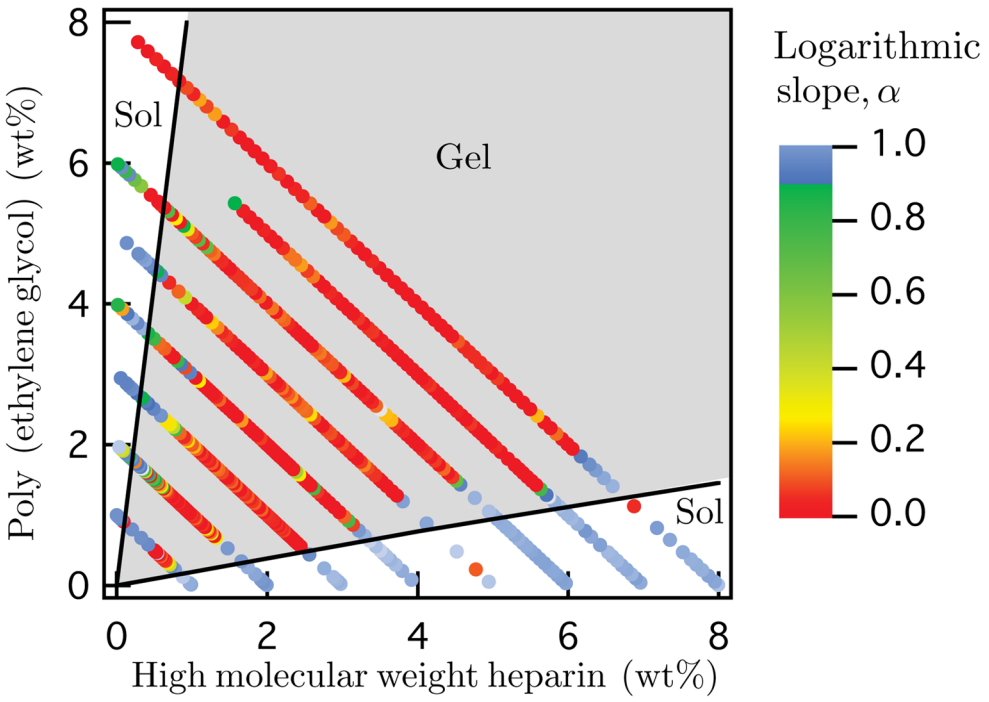

Figure 3.
Gelation state diagram measured using μ^2rheology black lines represent the upper and lower Flory-Stockmayer limits.

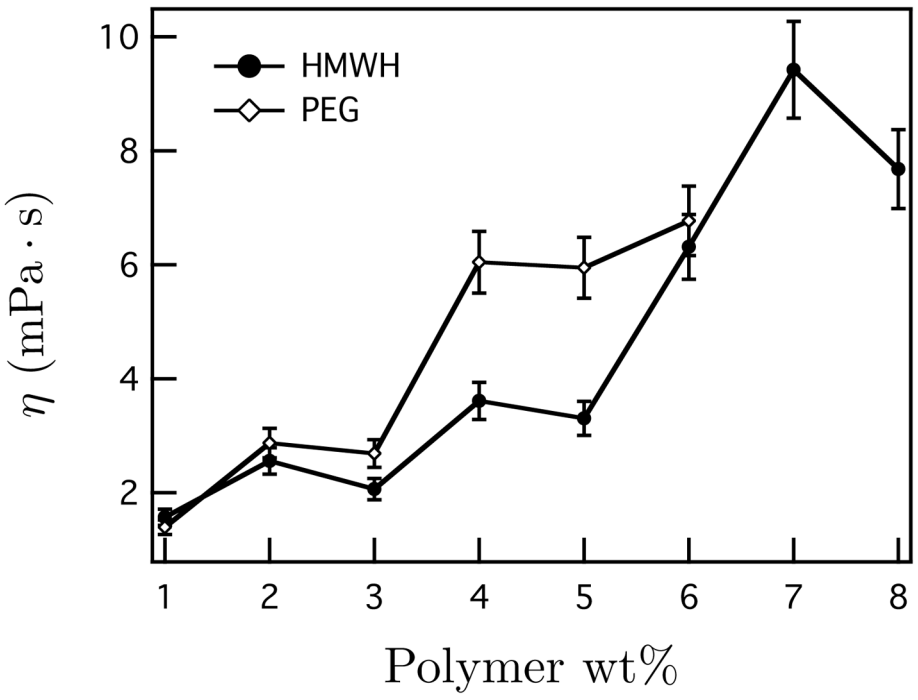

Figure 4.
Viscosity of HMWH and PEG measured using μ^2rheology. The bars indicate the inherent error of MPT measurements.